Elastic property changes of bitumen reservoir during steam injection

Ayato Kato, University of Houston, Shigenobu Onozuka, JOGMEC, and Toru Nakayama, JAPEX*

Summary

Elastic property changes of bitumen reservoir during steam injection have been poorly understood. We measured and analyzed ultrasonic velocities of bitumen-saturated sediments (oil sands) and then obtained a relation of the velocities with temperature and pressure individually. We also investigated validity of the Gassmann equation for predicting velocity changes. We combined the laboratory measurement results to obtain a sequential rock physics model that can predict the velocity changes induced by the steam injection.

Introduction

One of the most effective methods for producing the bitumen in Canada is the Steam-Assisted Gravity Drainage (SAGD) method. It makes the bitumen flowable by heating it with injected steam and reducing its viscosity. The steam movement is highly influenced by complex substructures in reservoir. Thus, the time-lapse seismic survey is expected to be powerful for monitoring the three-dimensional steam movement. However, the difficulties of making quantitative interpretation of the time-lapse seismic data remain because there has been no model of relating seismic velocities of oil sands directly with reservoir parameters (temperature, pressure, and pore fluid changes). In this study, we measured ultrasonic velocities of the oil sands and propose a practical model which can predict sequential seismic velocity changes during the steam injection.

Oil Sands Samples

We acquired whole cores from the oil sands reservoir in the Japan Canada Oil Sands Limited (JACOS) Hangingstone SAGD operation area, where the time-lapse seismic data had been acquired (the baseline survey in 2002 and the repeat survey in 2006 (Nakayama et al. (2006)). The oil sands samples were high-porous clean sands with small amounts of clay. We cut the whole cores into blocks and carefully whittled four plug samples from the blocks by a lathe. Next, the plug samples were trimmed in order to be held firmly with transducers. The four plug samples were 1.5 inches in diameter and approximately 1 inch in length. We measured the P- and S-wave velocities for the plug samples by the pulse-transmitted method with frequency of 0.5 MHz.

Pressure Dependence

The P- and S-wave oil sands velocities were measured under several pressure conditions at a constant temperature of 10 ˚C, which corresponds to the reservoir temperature before the steam injection. Figure 1 shows the velocities as a function of differential pressure, which is confining pressure (900 psi) minus pore pressure. We observed that the P- and S-wave velocities gradually decrease with decreasing differential pressure. Appling the natural logarithm as a fitting curve, we obtained a relationship between the velocities and pressure.

$$
\begin{aligned}
V_p &= 0.0593 \cdot Log(900 - P_{pore}) - 0.375 + V_{P0} \\
V_S &= 0.0780 \cdot Log(900 - P_{pore}) - 0.495 + V_{S0}
\end{aligned}
\qquad (1)
$$

where P_{pore} is pore pressure (psi), V_P and V_S are P- and S-wave velocities (km/s) respectively, and V_{P0} and V_{S0} are P- and S-wave velocities (km/s) at the initial condition (pore pressure of 300 psi and temperature of 10 ˚C) respectively. The solid lines in Figure 1 represent Equation 1. The pore pressure increase from 300 to 700 psi induced by the steam injection causes velocity decrease; 65 m/s for *Vp* and 86 m/s for *Vs*.

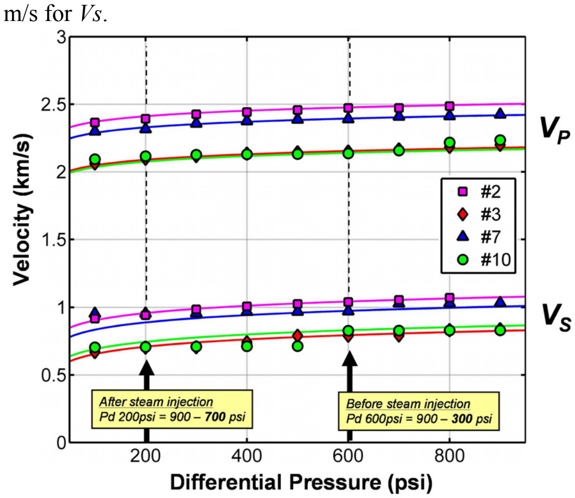

Figure 1: P- and S-wave velocities of the oil sands as a function of differential pressure at constant temperature of 10˚C. The numbers (#2, #3, #7, and #10) represent sample number of the measured oil sands.

Temperature Dependence

We also measured the P- and S-wave oil sands velocities as a function of temperature at a constant pore pressure of 700 psi. A slope of the velocities to temperature significantly changes at around 30 ˚C. In the lower temperature range the P- and S-wave velocities steeply decrease, where bitumen filled in the pores works as a quasi-solid to stiffen the rock grain frame moduli (Han et al., 2006). We divided the velocities at a given temperature by the initial velocities at 10 ˚C to obtain normalized velocities (Figure 2). The normalized velocities were fitted with two linear lines which connect to each other at 30 ˚C.

$T < 30$ ˚C

$$V_P / V_{P1} = -0.00550 \cdot T + 1.06$$
$$V_S / V_{S1} = -0.0190 \cdot T + 1.19$$

(2)

$T \geq 30$ ˚C

$$V_P / V_{P1} = -0.00168 \cdot T + 0.940$$
$$V_S / V_{S1} = -0.000640 \cdot T + 0.639$$

where T is temperature (˚C), V_{P1} and V_{S1} are P- and S-wave velocities (km/s) respectively at temperature of 10 ˚C and pore pressure of 700 psi. In accordance with Equation 2, the normalized P- and S-wave velocities at 80 ˚C are 0.81 and 0.59, respectively.

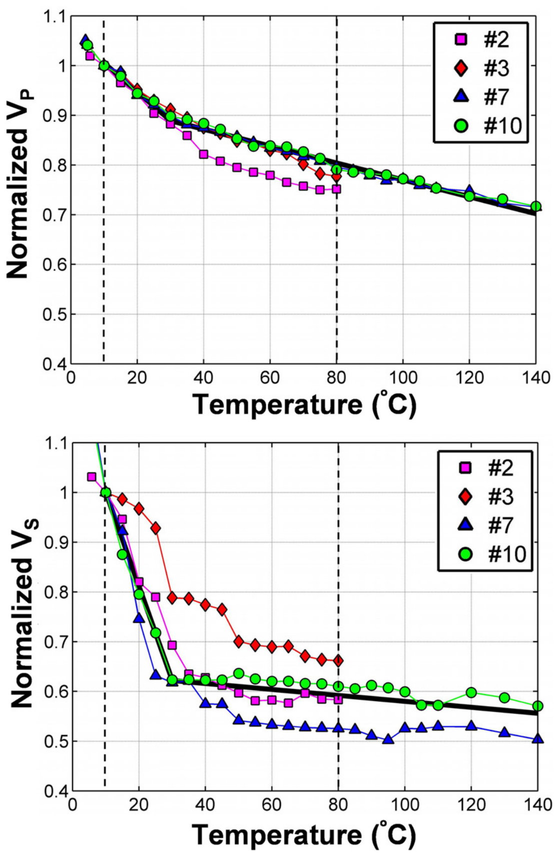

Figure 2: Normalized P- and S-wave velocities of the oil sands as a function of temperature at constant pore pressure of 700 psi. The black solid lines represent Equation 2.

Application of the Gassmann Equation

Dry frame moduli were calculated from the ultrasonic laboratory measurement data based on the Gassmann equation in order to investigate its validity for predicting velocity changes caused by the steam injection. Porosity and water saturation were determined to be 37 % and 19.6 % respectively by petrophysical analysis of the well logs. Mineral bulk modulus was assumed to be 35.5 GPa, taking into account the small amounts of clay. The bulk modulus and density of the bitumen were calculated from the FLAG program developed in Fluids/DHI consortium and its shear modulus was assumed to be zero. The calculated shear modulus rapidly decreases from 10 to 30 ˚C, and then gradually decreases from 30 to 70 ˚C (Figure 3). The bulk modulus also obviously decreases at lower temperatures than 80 ˚C. The significant depression of the dry frame moduli at the lower temperatures can be interpreted as: (1) the bitumen with higher viscosity stiffens the grain contacts, (2) the Gassmann equation fails because the bitumen has substantial rigidity, or (3) there is an effect of velocity dispersion between the low frequency of the Gassmann equation and high frequency of the ultrasonic measurement. On the other hand, they remain at approximately constant values at temperatures greater than 80 ˚C. The unvaried dry frame moduli at the higher temperatures implies that the Gassmann equation would be applicable for predicting velocity changes.

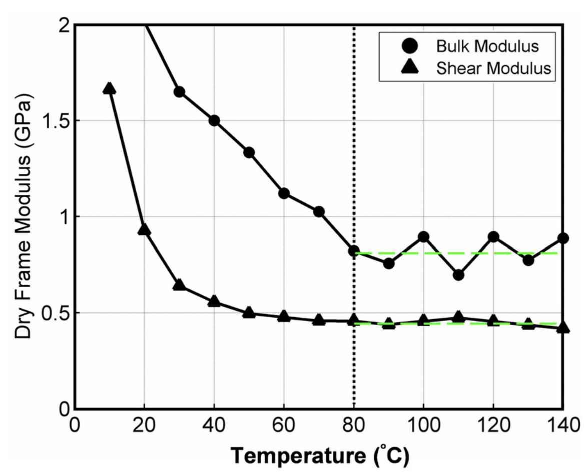

Figure 3: Dry frame moduli of the oil sands (sample #7) at pore pressure of 700 psi.

In order to justify the above hypothesis, we calculated the velocity changes caused by fluid property changes based on the Gassmann equation. In the calculation, dry frame moduli were assumed to be constant (K and G are 0.80 GPa and 0.48 GPa respectively) even though temperature varies. The calculated velocities were fairly consistent with the measurement at higher temperatures than 80 ˚C. This result encourages the use of the Gassmann equation for predicting velocity changes caused by any pore fluid property changes (due to not only temperature changes but also water saturation and phase changes) at the higher temperatures until the rock frame undergoes direct damage from the steam injection.

Sequential Rock Physics Model

We combined the laboratory measurement results to obtain a sequential rock physics model that can predict velocity changes induced by the steam injection:

1. *Ppore 300 psi → 700 psi (at T = 10 ˚C)*

$$V_p = 0.0593 \cdot Log(900 - P_{pore}) - 0.375 + V_{P0}$$
$$V_S = 0.0780 \cdot Log(900 - P_{pore}) - 0.495 + V_{S0}$$

2. *T 10 ˚C → 30 ˚C (at Ppore = 700 psi)*

$$V_p = (-0.00550 \cdot T + 1.06) V_{P1}$$
$$V_S = (-0.0190 \cdot T + 1.19) V_{S1} \qquad (3)$$

3. *T 30 ˚C → 80 ˚C (at Ppore = 700 psi)*

$$V_p = (-0.00168 \cdot T + 0.940) V_{P1}$$
$$V_S = (-0.000640 \cdot T + 0.639) V_{S1}$$

4. *T ≥ 80 ˚C (at Ppore = 700 psi)*
   The Gassmann equation can predict velocity changes
   Fluid properties are based on the FLAG program

where V_{P1} and V_{S1} are P- and S-wave velocities (km/s) respectively at pore pressure of 700 psi and temperature of 10 ˚C, which can be calculated from the first relations between the velocities and pressure. Once steam is injected into the reservoir, the pressure front rapidly spreads to the periphery, and the temperature front follows it. The P- and S-wave velocities decrease due to the pore pressure increase as a natural logarithm relation with differential pressure. After the pressure change, the velocities decrease with increasing temperature as a linear relation with a change in the slope at 30 ˚C as shown in Figure 2. The velocities at temperatures greater than 80 ˚C can be calculated by the Gassmann equation with the FLAG program.

Velocity Dispersion

We made a comparison between the surface seismic interval velocity and the sonic log interval velocity for the oil sands reservoir. The seismic interval velocities were calculated from two-way time differences between two seismic horizons which nearly correspond to the reservoir top and bottom at the well locations. The sonic interval velocities were calculated from time-depth relations of the corresponding reservoir interval. Both the interval velocities were not affected by the steam injection because the data used for the calculation had been acquired prior to it. From the comparison, the seismic interval velocity was estimated to be 7.6% lower than the one of sonic log on average.

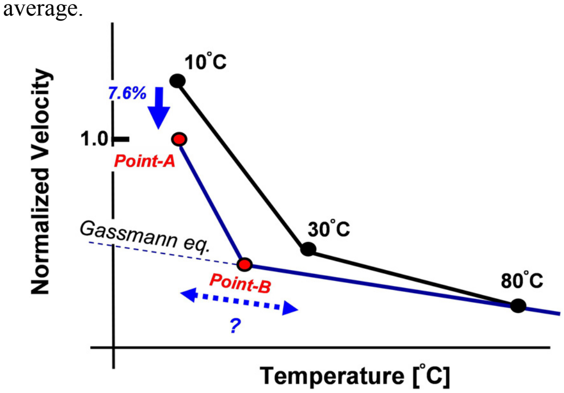

Figure 4: Schematic illustration of a practical method for calibrating the velocity dispersion.

We propose a practical method for calibrating the velocity dispersion (Figure 4). As stated before that the Gassmann equation is applicable at temperatures greater than 80 ˚C for the high frequency ultrasonic laboratory measurements. When we apply the Gassmann equation to the surface seismic data, we assume that the temperature limitation of the Gassmann equation can extend to lower temperatures until the dry frame moduli change or the bitumen has a substantial rigidity. In addition, we have the average value of the interval velocity difference between the surface seismic and the sonic data at the initial condition. The seismic velocity at the initial condition is estimated from the sonic velocity with the average velocity dispersion. We transform them into normalized velocities and connect the initial point (Point-A) with the temperature limitation of the Gassmann equation (Point-B) by a linear line. However, we do not know the temperature limitation. Fortunately, the Point-B can only move in a small range from 10 to 30 ˚C. Assuming the temperature limitation is 25 ˚C, we modified the coefficients associated with the temperature dependence in Equation 3 and obtained new sequential rock physics model which is adapted for low frequency band of the surface seismic.

1. *Ppore 300 psi → 700 psi (at T = 10 ˚C)*

$$V_p = 0.0593 \cdot Log(900 - P_{pore}) - 0.375 + V_{P0}$$
$$V_S = 0.0780 \cdot Log(900 - P_{pore}) - 0.495 + V_{S0}$$

2. *T 10 ˚C → 25 ˚C (at Ppore = 700 psi)*

Elastic property changes of bitumen reservoir during steam injection

$$V_p = (-0.00433 \cdot T + 1.04)V_{P1}$$
$$V_S = (-0.0239 \cdot T + 1.24)V_{S1} \quad (4)$$

3. *$T \geq 25$ ˚C (at Ppore = 700 psi)*
   The Gassmann equation can predict velocity changes. Fluid properties are based on the FLAG program.

Sequential Elastic Property Changes

To understand elastic property changes of the oil sand reservoir during steam injection, we represented the sequential reservoir conditions using 23 steps (Figure 5). Pore pressure change is caused from step 1 to 5 followed by temperature change from step 6 to 23. In addition, adjacent to the injector well, bitumen is replaced by hot water at step 18 and water phase changes from liquid to steam at step 21.

Step 1–5 : pore pressure increases (from 300 to 700 psi)
Step 6–23 : temperature increases (from 10 to 300 ˚C)
Step 18 : bitumen is replaced by hot water at 200 ˚C
Step 21 : phase changes from liquid to steam at 260 ˚C

Assuming that the sonic P- and S-wave velocities at the initial condition (step 0) are 2.4 km/s and 1.0 km/s respectively, the seismic velocities at step 1 are calculated by applying the average velocity dispersion (Figure 5 and 6). The P- and S-wave velocities decrease in the first pressure change from step 1 to 5. In the temperature increase from step 5 to 8, the P- and S-wave velocities decrease and the Vp/Vs ratio significantly increases because amount of decrease of the S-wave velocity is relatively larger than the P-wave velocity. After step 8 (25 ˚C), the P-wave velocity continues to decrease while the S-wave velocity remains virtually constant (because shear modulus is constant). At step 18 (200 ˚C), where the movable bitumen is largely replaced by the hot water (Sw from 20 % to 80%), the P-wave velocity slightly increases because the hot water has a faster P-wave velocity than one of the bitumen. Finally, the water phase changes from liquid to steam at step 21 (260 ˚C), leading to significant P-wave velocity drop (while the S-wave velocity slightly increases because of density decrease).

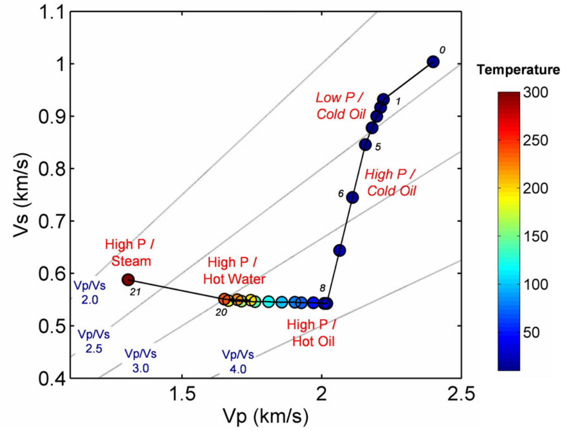

Figure 6: Crossplot between Vp and Vs based on the conditions of Figure 5.

Conclusions

We measured and analyzed the ultrasonic velocities of the oil sands cores acquired from the SAGD operation area and constructed the sequential rock physics model. The practical method for calibrating the velocity dispersion was proposed. The elastic property changes induced by the steam injection were predicted.

Acknowledgments

We wish to thank JACOS, JAPEX, and JOGMEC for permission to publish this paper. We also thank the corporate sponsors of the Fluids/DHI consortium.

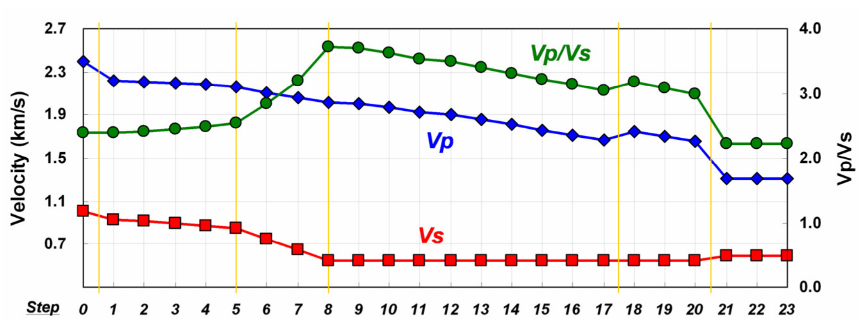

Step	0	1	2	3	4	5	6	7	8	9	10	11	12	13	14	15	16	17	18	19	20	21	22	23
Pp (psi)	300	300	400	500	600	700	700	700	700	700	700	700	700	700	700	700	700	700	700	700	700	700	700	700
T (˚C)	10	10	10	10	10	10	15	20	25	30	50	70	80	100	120	140	160	180	200	220	240	260	280	300
Sw (%)	20	20	20	20	20	20	20	20	20	20	20	20	20	20	20	20	20	20	80	80	80	80	80	80

Figure 5: Sequential P- & S- wave velocity and Vp/Vs ratio changes induced by steam injection.

EDITED REFERENCES

Note: This reference list is a copy-edited version of the reference list submitted by the author. Reference lists for the 2008 SEG Technical Program Expanded Abstracts have been copy edited so that references provided with the online metadata for each paper will achieve a high degree of linking to cited sources that appear on the Web.

REFERENCES

Han, D., J. Liu, and M. Batzle, 2006, Acoustic property of heavy oil-measured data: 76th Annual International Meeting, SEG, Expanded Abstracts, 1903–1907.

Nakayama, T., A. Takahashi, and H. Mochinaga, 2006, Time-lapse seismic survey in the oil sands area—JACOS SAGD Operation Area, Athabasca, Canada—Model Study and Data Acquisition: The 8th SEGJ International Symposium, SEGJ Proceedings, 355–358.